# Multicolor Imaging and Anticancer Effect of a Bifunctional Silica Nanosystem Based on the Complex of Graphene Quantum Dot and Hypocrellin A

*Lin Zhou[a], Lin Zhou[b], Xuefeng Ge[a], Jiahong Zhou[a,*], Shaohua Wei[a,*], Jian Shen[a]*

a College of Chemistry and Materials Science, Analysis and Testing Centre, Jiangsu Key Laboratory of Biofunctional Materials, Jiangsu Collaborative Innovation Centre of Biomedical Functional Materials, Key Laboratory of Applied Photochemistry, Nanjing Normal University, Wenyuan Road No.1, 210023, Nanjing, China.
b School of Chemistry & Chemical Engineering, Jiangsu University, Xuefu Road No. 301, 212013, Zhenjiang, China.

**Chemicals.**

The ultra small graphene oxide quantum dots (average size = 1-2 nm) were purchased from Nanjing XFNANO materials Tech Co. Ltd. 9,10-anthracenedipropionicacid (ADPA) was from Sigma; 3-[4,5-dimethylthiazol-2-yl]-2,5-diphenyl tetrazoliumbromide (MTT) were from Amosco; Dulbecco's minimum essential medium (DMEM) and fetal bovine serum (FBS) were from Gibico. 3-(2-Aminoethylamino)-propyltriethoxysilane was from TCI. All the other chemicals were used without further purification.

**HA/GQD and HA/GQD/SiO$_2$ preparation.**

In a typical experiment, 100 μL HA (15 mM in N,N-dimethyl-Formamide, DMF) was dissolved in 20 mL Millipore™ water, and mixed with 200 μL GQD aqueous suspension (20 mg/mL) at room temperature for 24 h with slow string to form HA/GQD complex.

20 mL HA/GQD/SiO$_2$ aqueous solution was prepared by improved sol-gel method. [1] Typically, above result HA/GQD complex aqueous solution was sonicated to disperse. Then, 100 μL 3-(2-aminoethylamino)-propyltriethoxysilane was added to above solution, and the resulting solution was stirred for about 1 h. After that, 1 mL of ammonium hydroxide (28%wt ammonia) was added and the system stirred for 24 h. At the end of the process, a red translucency indicated the formation of HA/GQD/SiO$_2$. Finally, the byproduct and ammonium hydroxide in the solution was removed by dialysis against water with a 12-14 kDa molecular weight cut off cellulose membrane for 12 h. The entire reaction was carried out at room temperature.

**Characterization.**

Transmission electron microscopy (TEM) was employed to determine the morphology and size of the aqueous dispersion, using a Hitachi H-7650 electron microscope, operating at an accelerating voltage of 120 kV. Ultraviolet-Visible (UV-Vis) absorption spectra were measured with a Varian Cary 50 spectrophotometer, where the light path length was 1 cm. The fluorescence spectra, lifetime of the fluorescence and time-resolved fluorescence spectroscopy (TRES) measurements were carried out in a Horiba Jobin Yvon Fluoro Max-4 time correlation single photon counting (TCSPC) system equipped with 450 and 570 nm nano-LED, The data were fitted using a reconvolution method of the instrument response function producing $X^2$ (Chi.Sq.) fitting values of 1-1.40. The HA/GQD is excited with a 370 nm nano-LED; it's TRES, with a 5-nm step, were recorded from 400 up to 700 nm by time gating the single photon counting detection system and scanning the emission spectrum. Microscopy

fluorescence images were acquired by an Nikon Ti Microscopy. The light source of Microscopy was a C-LHG1HG-100W Mercury Lamp. DAPI filter block was consisted with a EX 340-380 nm excitation filter and BA 435-485 nm barrier filter. FITC filter block was consisted with a EX 465-495 nm excitation filter and BA 515-555 nm barrier filter. TRITC filter block was consisted with a EX 540-525 nm excitation filter and BA 605-655 nm barrier filter. In our experiments, the exposure duration under DAPI, FITC and TRITC filter were 120, 150 and 80 ms, separately. Circular dichroism (CD) spectra of the aqueous solutions of samples were recorded using a quartz cuvette in an Applied Photophysics Chriascan spectropolarimeter. The surface charge of samples was measured with Malvern Zetasizer Nano 90 measurements in aqueous system. PSs exciting light source, used in all PDT experiments, was a 470 nm light emitting diode (LED) (2 W). All of the experiments was carried out in aqueous solution system.

**Extracellular $^1O_2$ detection.**

ADPA can be bleached by $^1O_2$ to its corresponding endoperoxide ADPAO$_2$, So, it can be used as $^1O_2$ generation detection sensor.[2] The reaction was recorded spectrophotometrically by detecting the decrease in absorbance intensity of $\lambda_{max}$ for ADPA (about 379 nm). Typically, 150 μL ADPA was mixed with 3 mL drug aqueous solution. Above solutions were irradiated with a 470 nm LED, and their UV-vis spectra were detected every 30 s.

*In vitro* **Cellular imaging of HA/GQD/SiO$_2$.**

Human cervical carcinoma cells (HeLa) were seeded in cell culture plate at the density of $1\times10^5$ cells/well in DMEM with 10 % FBS (5% CO$_2$, 37℃) for 24 h. Then, serum free medium with HA/GQD/SiO$_2$ (20 uM, calculated by HA) was replaced on the plate. After 4 h incubation in incubator, cells were washed with PBS (pH=7.4) three times and monitored by fluorescence microscopy through three filters: (1) 365 nm excitation, DAPI filter; (2) 470 nm excitation, FITC filter; and (3) 546 nm excitation, TRITC filter.

*In vitro* **PDT studies with tumor cells.**

HeLa cells ($5\times10^5$ cells/well) were seeded in 96-well plates. 24 h later, serum free medium with 4 μM different drugs (calculated by HB), including HA, HA/GQD and HA/GQD/SiO$_2$ was replaced on the plates. GQD and SiO$_2$ as control also treated cells. The cells were divided into two groups: (1) cells were placed in dark for 24 h in incubator; (2) cells were irradiated by 470 nm LED after 4 h incubation and then putted back to incubator for 20 h incubation. Finally, cell viability was measured using MTT assay.

**Statistical analysis.**

All the *in vitro* experiments data are presented in this article as mean result ± SD. Statistical differences were evaluated using the *t* test and considered significant at $P < 0.05$ level. All figures shown in this article were obtained from three independent experiments with similar results.
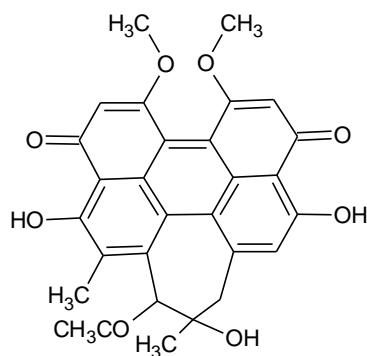
**Scheme S1.** Molecular structure of HA.

GQD has two aromatic planes and therefore is capable of adsorbing aromatic compounds. This kind of binding is physisorption, mainly via π-π stacking and hydrophobic interactions as stated previously by others. [3] To improve the formation of HA/GQD complex, the UV-Vis and CD spectra were employed to monitor the interaction between HA and GQD. Figure S1A shows the absorption spectra of HA, GQD and HA/GQD in aqueous solution. GQD without HA show virtually no absorption in the range of 400~750 nm. The HA spectrum exhibits strong absorption at this region. The peak I was due to the π-π* transition of HA; [4] the peak II and III was assigned to the formation of intramolecular hydrogen bonding between -OH and C=O in HA. [5] UV-Vis spectrum of GQD/HA was similar with HA, indicating that there is no obvious changes in the HA chromophore after carried. [6] Peak I intensity increasing possibly can be ascribed to the π-π transitions of electrons of the aromatic rings of HA when adding HA to GQD suggests that a π-π interaction occurred between the GQD and HA.[7] Peak II and III intensity increasing possibly due to the intermolecular hydrogen bond between -OH or =O of HA and -COOH or -OH of GQD.

To verify these hypotheses, CD spectra was analysis in Figure S1B. In the case of chromophores having chiral centers, a CD signal arises because of biased interchromophore aggregation leading to organized assemblies. [8] In the present case, CD was used to support that there is interaction between HA and GQD. HA have three positive CD cottons and two negative cottons because of its chirality property. After interacting with GQD, all of the positive cottons were increased and the negative cottons were decreased, which indicated that there are strong interaction between HA and GQD, which possibly because after noncovalent with GQD, the noncoplanar property was HA was greatly decreased due to the strong π-π stacking interaction between HA and GQD. [9]
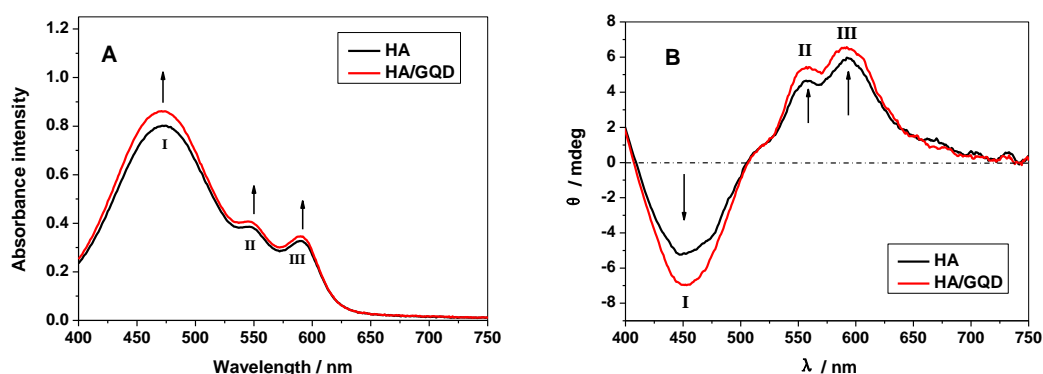


**Fig. S1.** UV-Vis (A) and CD (B) pattern changing of HA after interacting with GQD.

Zeta potential values of GQD and HA is -11.2 ± 0.1 and -8.1 ± 0.3 mV, separately. With adding HA, the zeta potential of the HA/GQD composites becomes more negative (-20.0 ± 0.6) due to the aggregation of negatively charged HA on the surface of GQD. [10] The samples all bear negative charges, which may be helpful for the high water disperse ability and solubility.[11]

The fluorescence property of GQD and HA/GQD droplet was studied by fluorescence microscope. The GQD is not provide one color imaging with DAPI filter but two with DAPI and FITC filter. HA can only provide one color imaging with TRITC filter. The fluorescence property of GQD droplet was studied by fluorescence microscope. As showed in Fig. SX, GQD droplet showed bright blue and green fluorescence. (Fig. S2A) As showed in Figure S2B, HA/GQD droplet showed bright blue, green and red fluorescence. This strong multicolor fluorescence property indicated such HA/GQD complex have potential to be used as multicolor imaging probe to mark cancer cells.
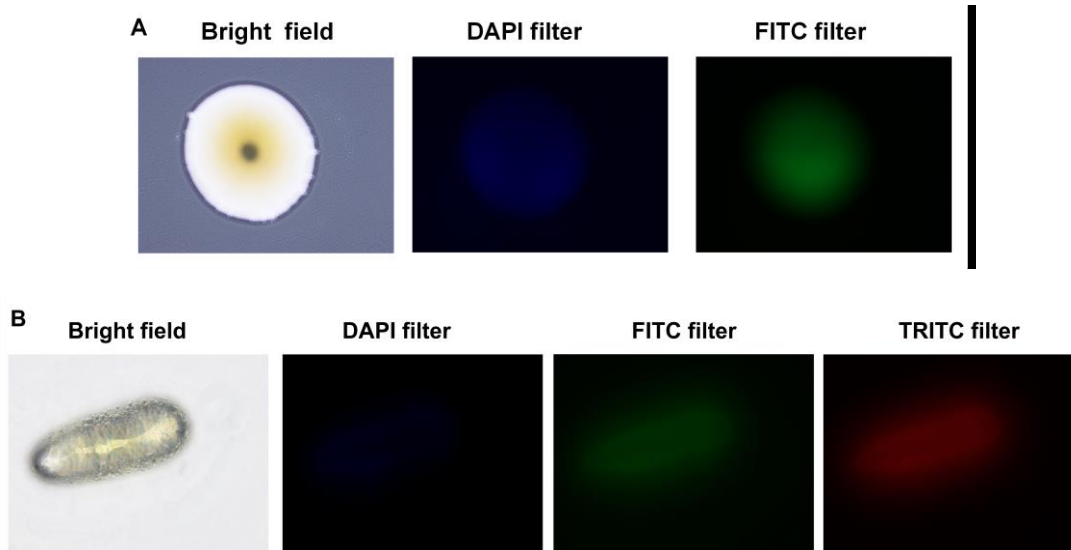
**Fig. S2.** The fluorescence microscope image of GQD (A) and HA/GQD (B) droplet.

To determine the GQD fluorescence quenching mechanism by HA, the nanosecond fluorescence lifetime of GQD was measured by the time correlation single photon counting (TCSPC) technique. As shown in Fig. 1B and Table S1, the fluorescence evolution of pure GQD can be nicely fitted by a biexponential function, which indicates two decay components, a fast one with the lifetime of 1.522 ns (96.03%) and a slow one with the lifetime of 6.891 ns (3.97%). With HA concentration increasing, a shorter component (0.643 ns, 24.80%) was appeared and the $\tau_{average}$ of systems was shapely decreased from 1.571 to 0.201 ns. Furthermore, the proportion of each component was also greatly changed. These results reveal the strong interaction between GQD and HA, which indicated that the contribution of dynamic quenching should be completely ruled out [12] and the static quenching constant was determined as $V = 13.15 \times 10^{-3}$ (mg/mL)$^{-1}$. Therefore, the dynamic quenching constant ($K_D$) can be negligible and the quenching process becomes purely static, which indicated the formation of HA/GQD complex.

**Table S1.** Fluorescence lifetime of GQD as a function of concentration of HA; [GQD] =50 μg/mL; [HA] / (1-6) = 0, 6, 12, 18, 24, 30 μg/mL.

|   | $\tau_1$ | $f_1$ | $\tau_2$ | $f_2$ | $\tau_3$ | $f_3$ | $\tau_{average}$ | Chi.Sq. |
|---|---|---|---|---|---|---|---|---|
| 1 | ----- | ----- | 1.522 ns | 96.03% | 6.891 ns | 3.97% | 1.571 ns | 1.187 |
| 2 | 0.634 ns | 24.80% | 1.800 ns | 67.39% | 9.340 ns | 7.80% | 1.292 ns | 1.054 |
| 3 | 0.402 ns | 32.41% | 1.827 ns | 59.18% | 11.33 ns | 8.41% | 0.879 ns | 1.186 |
| 4 | 0.235 ns | 41.03% | 1.714 ns | 50.61% | 12.91 ns | 8.35% | 0.489 ns | 1.197 |
| 5 | 0.165 ns | 53.11% | 1.714 ns | 40.19% | 13.48 ns | 6.69% | 0.289 ns | 1.162 |
| 6 | 0.136 ns | 65.36% | 1.680 ns | 29.62% | 10.05 ns | 5.02% | 0.201 ns | 1.073 |

If there is energy transfer process from GQD to HA, the energy transfer efficiency is typically measured using the relative fluorescence intensity of the donor, in the absence ($F_D$) and presence ($F_{DA}$) of acceptor based on Fig. 1A: [12]

$$E = 1 - \frac{F_{DA}}{F_D}$$

The energy transfer efficiency can also be calculated from the lifetime these respective conditions ($\tau_{DA}$ and $\tau_D$) based on Fig. 1B: [13]

$$E = 1 - \frac{\tau_{DA}}{\tau_D}$$

So,

$$E = 1 - \frac{\tau_{DA}}{\tau_D} = 1 - \frac{F_{DA}}{F_D}$$

However, the energy transfer efficiency is typically measured using the relative fluorescence intensity of the donor, in the absence and presence of acceptor was 27.50%; but the energy transfer efficiency been calculated from the lifetime these respective conditions was 87.21%. Reports indicated that this increased contribution might be ascribed to the quenching by HA through electron transfer. Therefore, there are both energy and electron transfer from GQD to HA and the energy transfer from GQD to HA is not effective at our experiment interaction ratio. So, When HA/GQD complex was formed, the high fluorescence property of GQD can be maintained.

Time-resolved fluorescence spectroscopy (TRES), a useful analysis of intermolecular interaction dynamics, of HA/GQD (Fig. S3) showed that after been excited by 370 nm nano-LED, the GQD portion of HA/GQD was quickly excited and showed fluorescence signal at about 450 nm. In the contrast, the excited HA signal (about 600 nm) was not detected until the exciting time was increased to 306.2-307.1 ns (1395-1399 channel, Time calibration = $2.194787 \times 10^{-10}$ s / channel). After that, with the GQD fluorescence intensity increasing, the fluorescence intensity of HA was gradually increased, which indicated that there are energy transfer from GQD to HA. After the GQD fluorescence intensity reached a maximum at 316.0-316.9 ns (1440-1444 channels) and then drops down, the fluorescence intensity of HA was only slightly increased and reached a maximum at 318.2-319.1 ns (1450-1454 channels). There was not obvious HA fluorescence intensity increasing when GQD was fully excited, which demonstrated that the energy transfer from GQD to HA is not effective. Furthermore, the energy transfer efficiency calculation results also improve that there are both energy and electron transfer from GQD to HA and the energy transfer from GQD to HA is not effective at our experiment interaction ratio. So, When HA/GQD complex was formed, the high fluorescence property of GQD can be maintained. Simultaneously, the affection from GQD to HA fluorescence property was also studied and the results indicated that the impact of GQD on HA was limited, which demonstrated that such interaction could not obviously affect the photo-exciting process of HA, and possibly do not affect its PDT effect (Fig. S3 and Table S2, ESI[†]).
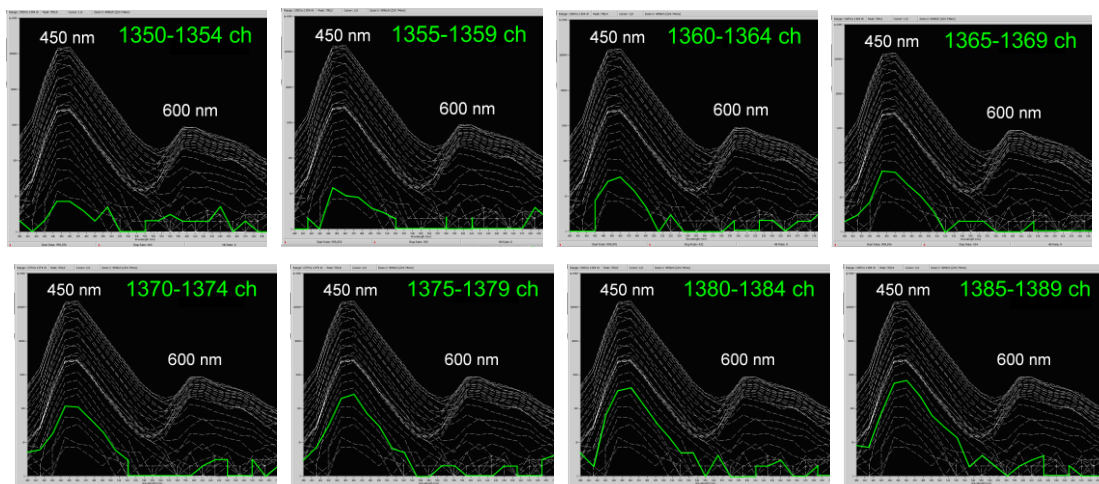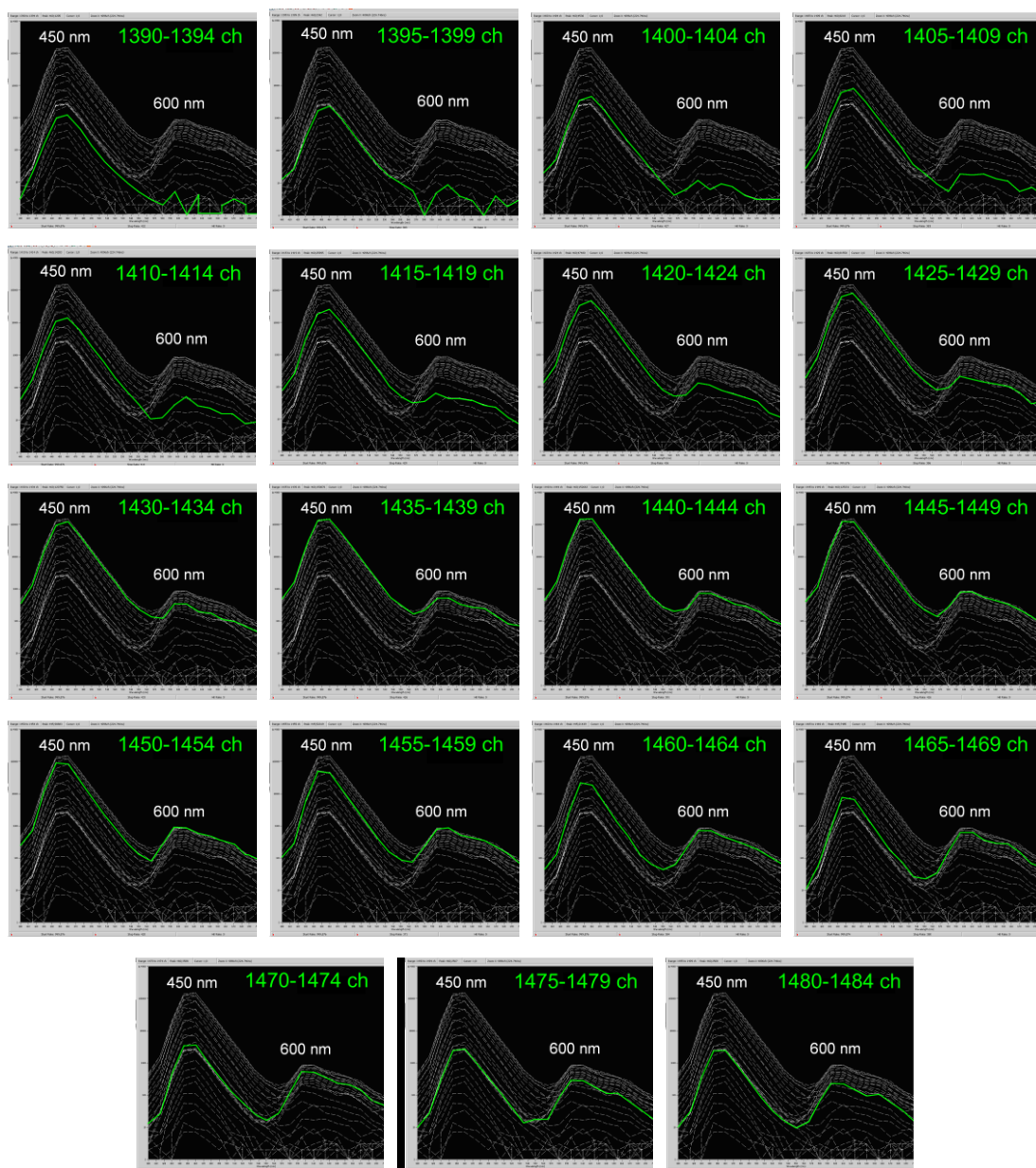
**Fig. S3.** TRES spectra of HA/GQD from 296.3-325.7 ns (1365-1484 channel, Time calibration = 2.194787×10$^{-10}$ s / channel) (X axis: wavelength / nm; Y axis: fluorescence intensity / counts)

To analysis the affection of such interaction to HA portion of HA/GQD complex, a 450 nm nano-LED was used excitation source, which predominately excites the HA portion (600 nm) of the hybrid in HA/GQD aqueous solution. As shown in Figure S4 and Table S2, the fluorescence evolution of pure HA can be fitted by a biexponential function, with a fast lifetime of 0.873 ns (44.09%) and a slow lifetime of 1.877 ns (55.91%). Besides, the fluorescence intensity of HA was slightly decreased after GQD was added. With increasing GQD concentrations, the fluorescence lifetimes, their proportion and intensity have slight change, which indicated that there are interaction between HA and GQD. These slight changing degree of fluorescence lifetime and intensity demonstrated that such interaction could not obviously affect the photo-exciting process of HA, and possibly do not affect its PDT effect.
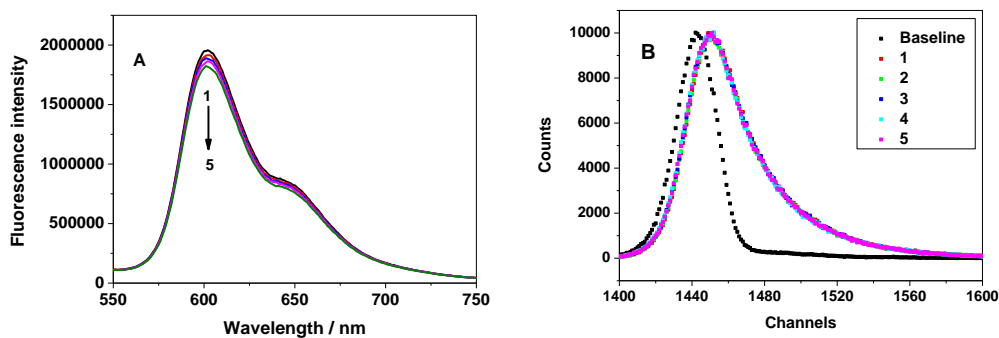
**Fig. S4.** (A) Time-resolved fluorescence decays for GQD in the absence and presence of HA; (B) Time-resolved fluorescence decays for GQD in the absence and presence of HA. [HA] = 5.00 μg/mL; [GQD] / (1-5) = 0.00, 6.25, 12.5, 18.75, 25.00 μg/mL.

**Table S2.** Fluorescence lifetime of HA as a function of concentration of GQD. [HA] = 5.00 μg/mL; [GQD] / (1-5) = 0.00, 6.25, 12.5, 18.75, 25.00 μg/mL.

|   | $\tau_1$ | $f_1$ | $\tau_2$ | $f_2$ | $\tau_{average}$ | Chi.Sq. |
|---|---|---|---|---|---|---|
| 1 | 0.873 ns | 44.09% | 1.877 ns | 55.91% | 1.245 ns | 1.299 |
| 2 | 0.821 ns | 38.09% | 1.815 ns | 61.91% | 1.242 ns | 1.268 |
| 3 | 0.817 ns | 36.75% | 1.786 ns | 63.25% | 1.244 ns | 1.255 |
| 4 | 0.790 ns | 38.09% | 1.758 ns | 64.47% | 1.225 ns | 1.333 |
| 5 | 0.755 ns | 34.31% | 1.755 ns | 65.69% | 1.207 ns | 1.299 |

GQD without HA show virtually no absorption in the range of 400-700 nm. The UV-vis absorption of HA/GQD and HA/GQD/SiO$_2$ are similar (Figure S5), indicating no obvious changes in the HA/GQD chromophore upon entrapment inside nanoparticles, which implied that HA/GQD are stable after been encapsulated inside silica nanoparticles. The slight changes are possibly because of the environment changes for HA/GQD.
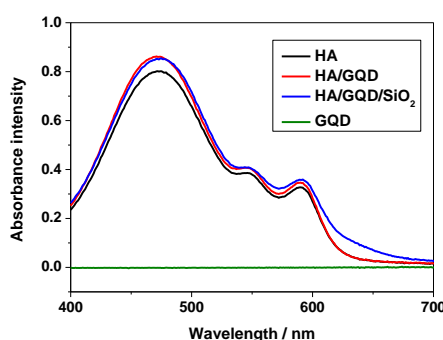


**Fig. S5.** The UV-Vis spectra of GQD, HA, HA/GQD and HA/GQD/SiO$_2$.

Photophysical properties of fluorescence is very important for fluorescence dye. The extinction coefficients ($E_{1cm}^{1\%}$) of HA and GQD in water were $3.0 \times 10^4$ and $1.2 \times 10^5$ cm$^{-1}$, separately. The fluorescence quantum yield (Φ) of GQD, HA, HA/GQD and HA/GQD/SiO$_2$ were detected. The fluorescence quantum yield of all samples were directly detected using Horiba Jobin Yvon Fluoro Max-4 spectrofluorometer equipped with an integrating sphere accessory [14] (Horiba Jobin Yvon). From Table S4, we can concluded that, after been encapsulated inside silica

nanoparticles, the fluorescence quantum yield of HA and GQD were both increased, which would helpful for their imaging.

**Table S3.** Three-dimensional fluorescence spectral characteristics of HA/GQD and HA/GQD/SiO$_2$.

| Samples | peak | Peak 1 | Peak 2 |
|---------|------|--------|--------|
| HA/GQD | Peak position ($E_X$/$E_M$) | 360 nm/456 nm | 455 nm/604 nm |
| | Fluorescence intensity | 29954 counts | 37240 counts |
| HA/GQD/SiO$_2$ | Peak position ($E_X$/$E_M$) | 360 nm/466 nm | 460 nm/606 nm |
| | Fluorescence intensity | 38607 counts | 120125 counts |

**Table S4.** Fluorescence quantum yield of GQD, HA, HA/GQD and HA/GQD/SiO$_2$.

| | GQD | HA | HA/GQD | | HA/GQD/SiO$_2$ | |
|---|---|---|---|---|---|---|
| | $E_x$=376 nm | $E_x$=480 nm | $E_x$=376 nm | $E_x$=480 nm | $E_x$=376 nm | $E_x$=480 nm |
| Φ | 14.49% | 4.02% | 7.31% | 3.88% | 15.22% | 11.97% |

Furthermore, we proposed that the encapsulation protection from silica nanopartilces could help fluorescence dyes minimize the fluorescence quenching effect by the massive complicated substances inside body. The imaging function of our nanoprticles was detected inside cells, where containing massive complicated substances including proteins, amino acids, inorganic salts, vitamins, lipid, carbohydrates and et al. So, we use cell-lysis to simulate physiological environment inside cells and detected the influence of fluorescence intensity for HA/GQD and HA/GQD/SiO$_2$ in cell-lysis. The fluorescence intensity of GQD, HA, HA/GQD and HA/GQD/SiO$_2$ was studied in this simulated physiological fluid (Fig. S6). The fluorescence intensity of HA and GQD was decreased when they were incubated in fluid, which indicated that some substances in this fluid could effectively quench the fluorescence of HA and GQD. In contrast, when they were encapsulated inside silica nanoparticles, such fluorescence quenching was significantly inhibited, especially for GQD.
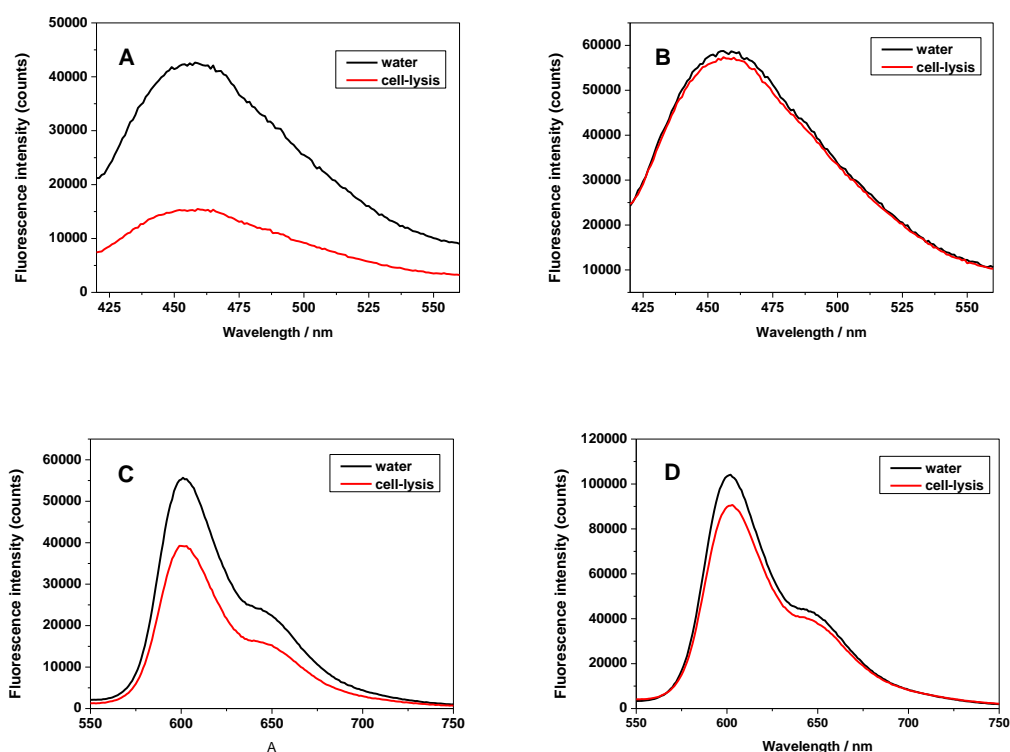
**Fig. S6.** The fluorescence spectra of HA/GQD and HA/GQD/SiO$_2$. (A) HA/GQD, $E_x$=360 nm; (C) HA/GQD, $E_x$=480 nm; (B) HA/GQD/SiO$_2$, $E_x$=360 nm; (D) HA/GQD/SiO$_2$, $E_x$=480 nm;

    The fluorescence intensity of GQD was partly reduced when HA/GQD complex was formed because of the energy transfer and electron transfer between GQD and HA. However, the fluorescence intensity of HA/GQD was significantly increased after been encapsulated inside silica nanoparticls, which can provides the guaranty for its imaging function.

    Furthermore, the present of GQD can effectively improve the monodisperse ability of HA in aqueous system because of the good water solubility of GQD. Such monodisperse property of HA/GQD is in favor of silica nanoparticle encapsulation process. And the HA/GQD/SiO$_2$ system would helpful to increase $^1O_2$ generation for its preventing quenching of energy transfer steps before $^1O_2$ generation (due to aggregation)

    It has been reported that the more uniform size distribution of carbon related quantum dots results in longer fluorescence lifetime. [15] And our results improve this report. The fluorescence lifetime of GQD, HA/GQD and HA/GQD/SiO$_2$ (at 450 nm) was detected using 370 nm nano-LED to analyze the lifetime change of GQD portion after interacting with HA and then encapsulating inside silica nanoparticles. Similar studies were also carried out to detect the lifetime changing of HA portion at 600 nm using 450 nm nano-LED. In accordance with the emission intensity, a similar trend is also observed in the emission decay dynamics, in which the lifetime of HA/GQD, both GQD and HA portion, was increased after been encapsulated inside silica nanopaticles (Figure S7 and Table S5).
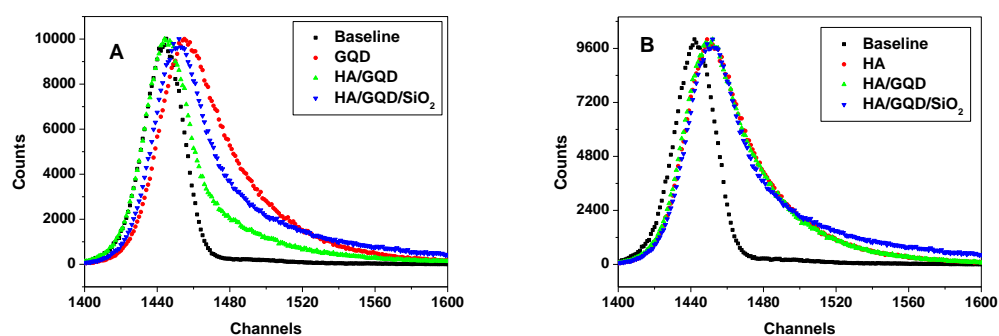


**Fig. S7.** Time-resolved fluorescence decays for HA, GQD, HA/GQD and HA/GQD/SiO$_2$ using 370 nm nano-LED (A) to detect GQD portion and 450 nm nano-LED (B) to detect HA portion.

**Table S5.** Average lifetimes for HA, GQD, HA/GQD and HA/GQD/SiO$_2$ using 370 nm nano-LED to detect GQD portion and 450 nm nano-LED to detect HA portion.

| Exciting wavelength | 370 nm LED for GQD (450 nm) | | | 450 nm nano-LED for HA (600 nm) | | |
|---|---|---|---|---|---|---|
| Sample | GQD | HA/GQD | HA/GQD/SiO$_2$ | HA | HA/GQD | HA/GQD/SiO$_2$ |
| $\tau_{average}$ (ns) | 1.571 | 0.201 | 1.062 | 1.245 | 1.207 | 1.355 |
| Chi.Sq. | 1.187 | 1.073 | 1.149 | 1.299 | 1.399 | 1.092 |

    GQD and SiO$_2$ without HA produced no change in the absorbance intensity of ADPA with time, confirming that the bleaching of ADPA in the presence of HA is caused by the generated $^1O_2$ and not by the irradiating light (Figure S8).
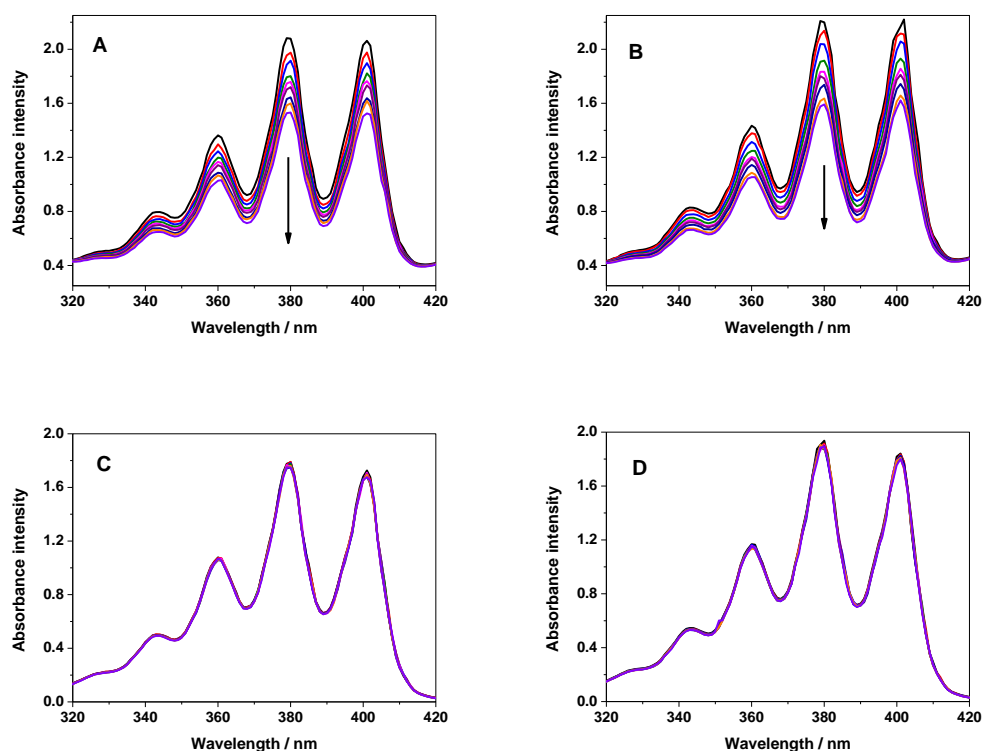
**Fig. S8.** Absorption spectra of HA (A), HA/GQD (B), GQD (C) and SiO$_2$ (D) system with ADPA were irradiated for 0, 30, 60, 90, 120, 150, 180, 210 and 240 s by light.

Photo-induced cancer cell morphology changing by HA, HA/GQD, HA/GQD/SiO$_2$, GQD and SiO$_2$ were shown in Figure S9. HeLa cells, which were treated with GQD or SiO$_2$ and irradiation, did not cause any significant change in cell morphology comparing with untreated cells. On the contrary, the morphology of HeLa cells, treated with HA, HA/GQD, HA/GQD/SiO$_2$ and irradiation, were drastically changed. These cells shrunk and appeared many membrane blebs. In addition, more cells were shrunk for HA/GQD/SiO$_2$ treated cells comparing with HA or HA/GQD treated one. These changes are associated with cell death and are apparently induced by the $^1$O$_2$ generated by these drugs.
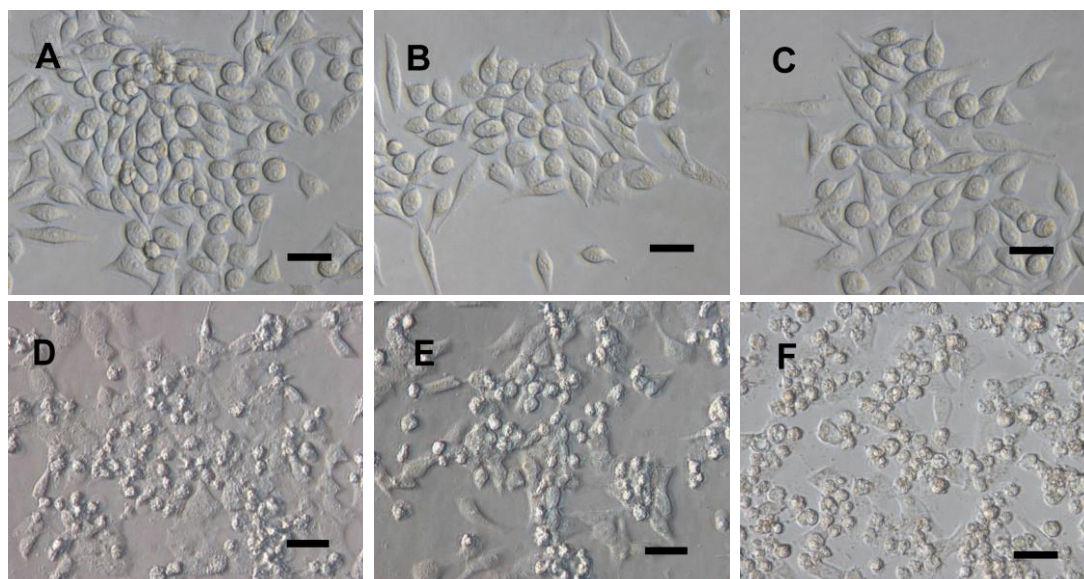
**Fig. S9.** Microscope images of HeLa cells. (A) Drug free cells were treated with irradiation; (B) Cells were treated with GQD and irradiation; (C) Cells were treated with SiO$_2$ and irradiation; (D) Cells were treated with HA and irradiation; (E) Cells were treated with HA/GQD and irradiation; (F) Cells were treated with HA/GQD/SiO$_2$ and irradiation (Bar=100 μm).

### References

1.  L. Zhou, J. H. Liu, J. Zhang, S. H. Wei, Y. Y. Feng, J. H. Zhou, B. Y. Yu, J. Shen, International Journal of Pharmaceutics 2010, **386**, 131.

2.  G. Charron, T. Stuchinskaya, D. R. Edwards, D. A. Russell, T. Nann, Journal of Physical Chemistry C 2012, **116**, 9334.

3.  L. M. Zhang, J. G. Xia, Q. H. Zhao, L. W. Liu, Z. J. Zhang, Small 2010, **6**, 537.

4.  J. H. Zhou, L. Zhou, C. Dong, Y. Y. Feng, S. H. Wei, J. Shen, X. S. Wang, Materials Letters 2008, **62**, 2910.

5.  L. Zhou, J. H. Liu, F. Ma, S. H. Wei, Y. Y. Feng, J. H. Zhou, B. Y. Yu, J. A. Shen, Biomedical Microdevices 2010, **12**, 655.

6.  P. Huang, J. Lin, X. S. Wang, Z. Wang, C. L. Zhang, M. He, K. Wang, F. Chen, Z. M. Li, G. X. Shen, D. X. Cui, X. Y. Chen, Advanced Materials 2012, **24**, 5104.

7.  C. Wang, C. Y. Wu, X. J. Zhou, T. Han, X. Z. Xin, J. Y. Wu, J. Y. Zhang, S. W. Guo, Scientific Reports 2013, **3**.

8.  (a)P. Chithra, R. Varghese, K. P. Divya, A. Ajayaghosh, Chemistry-an Asian Journal 2008, 3, 1365; (b)R. S. Stoll, N. Severin, J. P. Rabe, S. Hecht, Advanced Materials 2006, **18**, 1271.

9.  L. Zhou, H. J. Jiang, S. H. Wei, X. F. Ge, J. H. Zhou, J. Shen, Carbon 2012, **50**, 5594.

10. P. Huang, C. Xu, J. Lin, C. Wang, X. S. Wang, C. L. Zhang, X. J. Zhou, S. W. Guo, D. X. Cui, Theranostics 2011, **1**, 240.

11. P. Huang, J. Lin, X. Wang, Z. Wang, C. Zhang, M. He, K. Wang, F. Chen, Z. Li, G. Shen, D. Cui, X. Chen, Advanced Materials 2012, **24**, 5104.

12. A. Ahmad, T. Kurkina, K. Kern, K. Balasubramanian, Chemphyschem 2009, **10**, 2251.

13. S. Bhattacharyya, M. K. Barman, A. Baidya, A. Patra, Journal of Physical Chemistry C 2014, **118**, 9733.

14. J. C. deMello, H. F. Wittmann. R. H. Friend. Adv. Mater. 1997, 9, 230; (b) X. J Tu, W. B. Chen, X. Q. Guo. Nanotechnology. 2011, 22, 095701.

15. C. W. Lai, Y. H. Hsiao, Y. K. Peng, P. T. Chou, Journal of Materials Chemistry 2012, **22**, 14403.